

**(Electronic Supplementary Information)**

**Theoretical evidence of water serving as a promoter for lithium superoxide  
disproportionation in Li-O<sub>2</sub> batteries**

Nannan Shan,<sup>1</sup> Paul C. Redfern,<sup>1</sup> Anh T. Ngo,<sup>1,2</sup> Peter Zapol,<sup>1</sup> Nenad Markovic,<sup>1</sup> Larry A.  
Curtiss<sup>1\*</sup>

<sup>1</sup> Materials Science Division, Argonne National Laboratory, Lemont, IL, 60439, USA

<sup>2</sup> Department of Chemical Engineering, University of Illinois at Chicago, Chicago, IL, 60607,  
USA

\*Larry A. Curtiss: [curtiss@anl.gov](mailto:curtiss@anl.gov)

The PBE<sup>1</sup> calculations were done with as implemented in the Vienna ab initio simulation package (VASP),<sup>2</sup> and with spin-polarization. The projector augmented wave (PAW)<sup>3</sup> method was used to represent the interaction between the core electrons and valence electrons, and the Kohn–Sham valence states (2s for Li; 2s2p for O) were expanded in plane wave basis sets up to a kinetic energy cutoff of 500 eV.  $\Gamma$ -point was used to sample the Brillouin zone. The iteration loop will exit once the energy and force are below  $10^{-6}$  eV and  $0.02$  eV/Å. A unit box with size of  $20 \times 20.2 \times 20.5$  Å<sup>3</sup> were applied. The implicit solvation effect was considered with the VASPsol code developed by Henning group.<sup>4-5</sup> The free energy of one species was calculated with

$$G = E_o + ZPE - TS + \int_0^T C_p dT,$$

where  $E_o$  represents the electronic energy obtained from DFT calculation,  $ZPE$  the zero-point energy,  $TS$  the entropic contributions, and  $\int_0^T C_p dT$  the heat capacity at a constant pressure. The  $G_{sol}$  donates the free energy with the solvation correction from the implicit model.

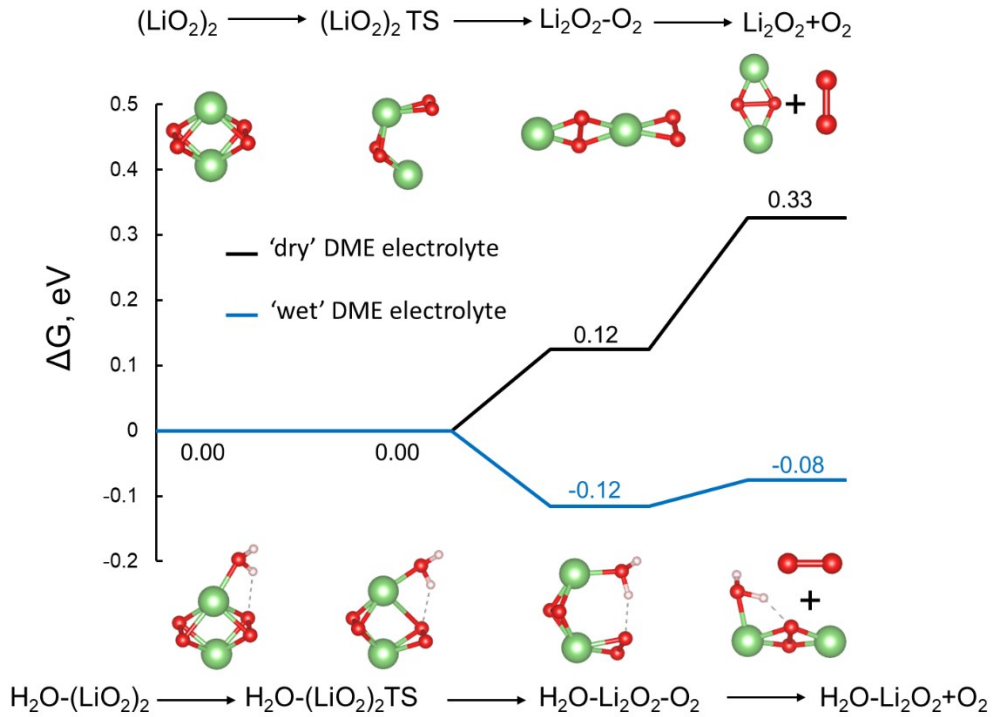


Figure S1. The reaction free energy landscape in ‘dry’ (black lines) and ‘wet’ (blue lines) DME

electrolyte for  $\text{LiO}_2$  disproportionation based on PBE(PW) method. The geometries of species in 'dry' and 'wet' electrolyte were depicted in top and bottom panels with the Li, O and H atoms in green, red and white, respectively.

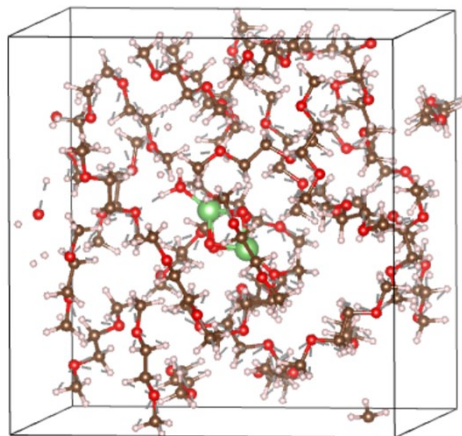


Figure S2. The configuration of a  $\text{H}_2\text{O}-(\text{LiO}_2)_2$  complex in the simulation box used in AIMD calculations. The Li, C, O, H atoms are displayed in green, brown, red and white, respectively. The blank lines represent the periodic boundaries.

The AIMD calculations were conducted on an Au(100) to evaluate reaction mechanisms as shown in Reactions (3-4). A three-layer ( $8 \times 8$ ) supercell of Au(100) was constructed with a 21 Å vacuum space filled with dimethoxyethane (DME) electrolyte with the density of 0.9 g/cm<sup>3</sup>, close to the reported experimental value of 0.87 g/cm<sup>3</sup>. The bottom layer was kept fixed at the Au bulk structure with a lattice value at 4.16 Å, while the top two layers of the Au(100) surface, the DME electrolyte molecules and reactants were free to move.

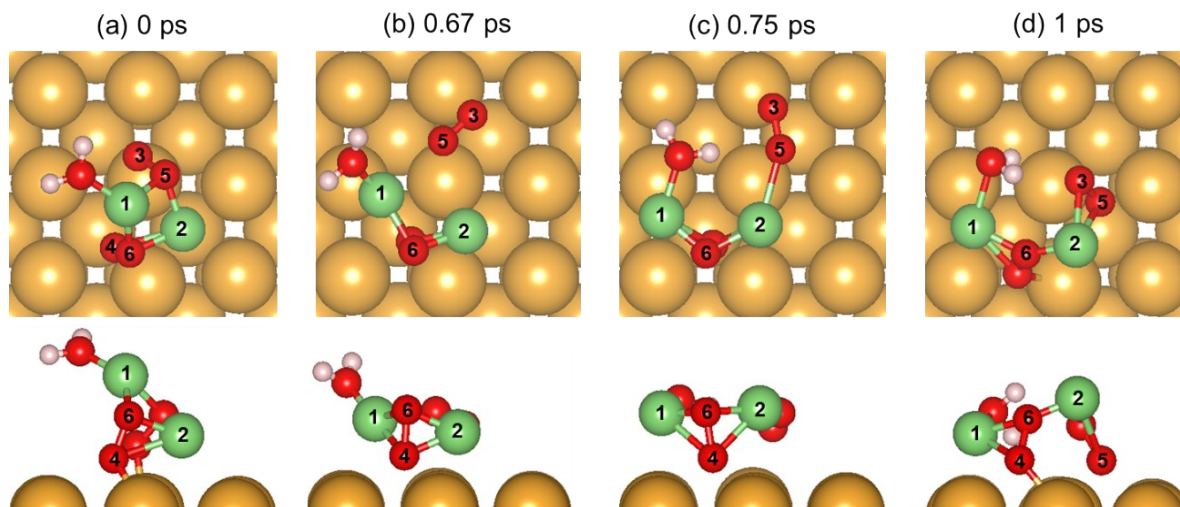


Figure S3. The structures at (a) 0ps, (b) 0.67ps, (c) 0.75ps, and (d) 1ps for  $\text{LiO}_2$  disproportionation reaction in ‘wet’ DME electrolyte obtained from AIMD calculations at 300K. The O, H, Li and Au atoms are in red, white, green, and gold, respectively. The top- and side-views are in upper and lower panels, respectively. All the DME solvent molecules were hidden for the visualization purpose. The Li and O atoms are labeled with numbers one to six for vision guidance.

The  $\text{LiO}_2$  disproportionation reaction as shown in Reaction (3) in ‘wet’ DME electrolyte was evaluated using AIMD calculations on Au(100) electrode at constant temperature, i.e. 300 K. The representative snapshots from AIMD calculations in ‘wet’ DME are displayed in Figure S3, the explicit DME molecules were removed for the visualization purpose. Two Li and four O atoms were labeled with No.1-6 for vision guidance. The initial structure was obtained from the optimized geometry at the ground state. The  $\text{H}_2\text{O}-(\text{LiO}_2)_2$  complex binds on two top sites of Au(100) with No.3 and No.4 oxygen atoms, as shown in Figure S3(a). Two hydrogen bonds between water and two DME molecules are invisible due to the hidden DME molecules. Starting from the initial  $\text{H}_2\text{O}-(\text{LiO}_2)_2$  complex, the  $\text{H}_2\text{O}-\text{Li}_2\text{O}_2$  and  $\text{O}_2$  are observed separating with a closest 2.56 Å distance between No.1 Li and No.5 O at 0.67 ps, and this distance keeps increasing along the reaction timeline, indicating the disproportionation reaction is happening, as described in Figure S3(b). At 0.75 ps, the separated  $\text{O}_2$  reattached onto the  $\text{H}_2\text{O}-\text{Li}_2\text{O}_2$  complex, forming a Li-O bond between No.2 Li and No.5 O with bond length of 2.45 Å (see Figure S3(c)). At 1 ps in Figure S3(d), both No.3 and No.5 oxygen atoms bind on No.2 Li atom, forming another configuration of the  $\text{H}_2\text{O}-(\text{LiO}_2)_2$  complex. In fact, as the AIMD simulation continued running up

to 2 ps, this reaction cycle is repeating by following with the similar configurations in Figure S3(d, b, c). The demonstrated AIMD calculations provide the theoretical evidence that the  $\text{H}_2\text{O}-(\text{LiO}_2)_2$  complex disproportionation to  $\text{H}_2\text{O}-\text{Li}_2\text{O}_2$  complex can happen on Au(100) surface in ‘wet’ DME electrolyte at 300K.

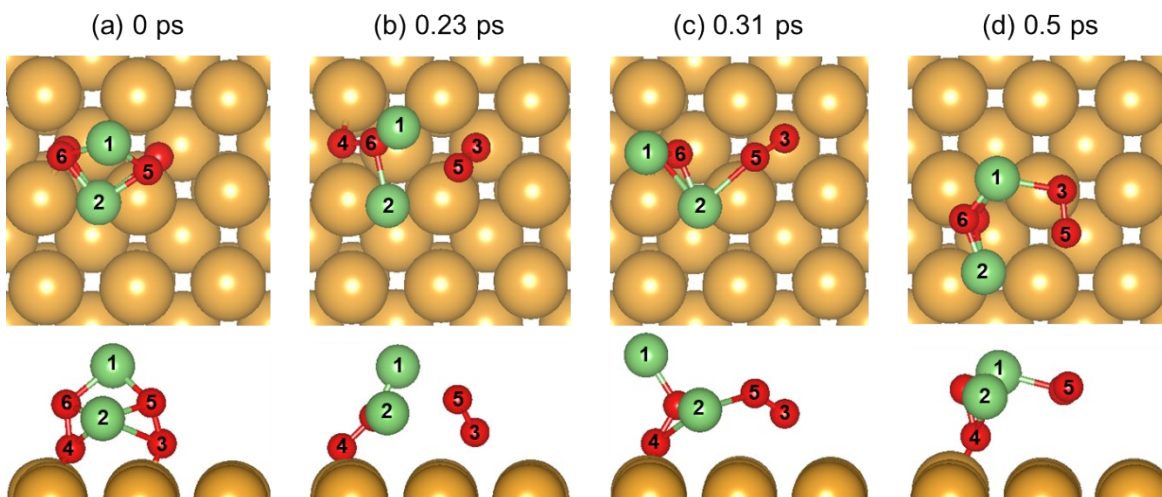


Figure S4. The structures at (a) 0ps, (b) 0.23ps, (c) 0.31ps, and (d) 0.5ps for disproportionation reaction from AIMD calculations at 300 K in ‘dry’ DME electrolyte. The O, H, Li and Au atoms are in red, white, green, and gold respectively. The top- and side-views are in upper and lower panels, respectively. All the DME solvent molecules were removed for the visualization purpose. The Li and O atoms are labeled with No.1-6 for vision guidance.

The AIMD simulation for  $\text{LiO}_2$  disproportionation reaction on Au(100) electrode was also performed in ‘dry’ DME electrolyte. The selected snapshots from AIMD calculations were depicted in Figure S4. Similarly the explicit DME molecules were removed for clear visualization and the Li and O atoms were labeled from one to six. The AIMD calculations began with the optimized structure, in which No.3 and No.4 oxygen bind on Au(100) surface (see Figure S4(a)). At 0.23 ps with geometry shown in Figure S4(b), an  $\text{O}_2$  separated from  $\text{LiO}_2$  dimer with a distance of 2.57 Å between No.1 Li and No.5 O and 2.64 Å between No.2 Li and No.5 O, which is treated as a sign showing the  $\text{LiO}_2$  dimer disproportionation was happening. At 0.31 ps, the  $\text{O}_2$  moved close to  $\text{Li}_2\text{O}_2$  and formed a Li-O bond with a bond length of 2.46 Å as depicted in Figure S4(c). Figure S4(d) exhibited the geometry of  $\text{Li}_2\text{O}_2-\text{O}_2$  complex with the 2.13 Å Li-O bond between

No.1 Li and No.3 O. The AIMD calculations kept running for 2 ps and the  $\text{Li}_2\text{O}_2/\text{O}_2$  and  $\text{Li}_2\text{O}_2\text{-O}_2$  complex appear repeatedly.

The adsorptions of  $\text{LiO}_2$  on Au(100), Au(111) and Au(110) surfaces were also calculated using VASP. The different adsorption sites of Au(100), Au(111) and Au(110) surfaces were tested and the adsorption energies ( $\Delta E$ ) were defined as,  $\Delta E = E_{\text{LiO}_2_{\text{ads}}} - E_{\text{clean\_surf}} - E_{\text{LiO}_2_{\text{gas}}}$ , where  $E_{\text{LiO}_2_{\text{ads}}}$ ,  $E_{\text{clean\_surf}}$  and  $E_{\text{LiO}_2_{\text{gas}}}$  are the calculated electronic energies of  $\text{LiO}_2$  on selected surface, clean surface,  $\text{LiO}_2$  in gas phase. The most stable geometries and corresponded adsorption energies on Au(100), Au(111) and Au(110) are displayed in Figure S5.

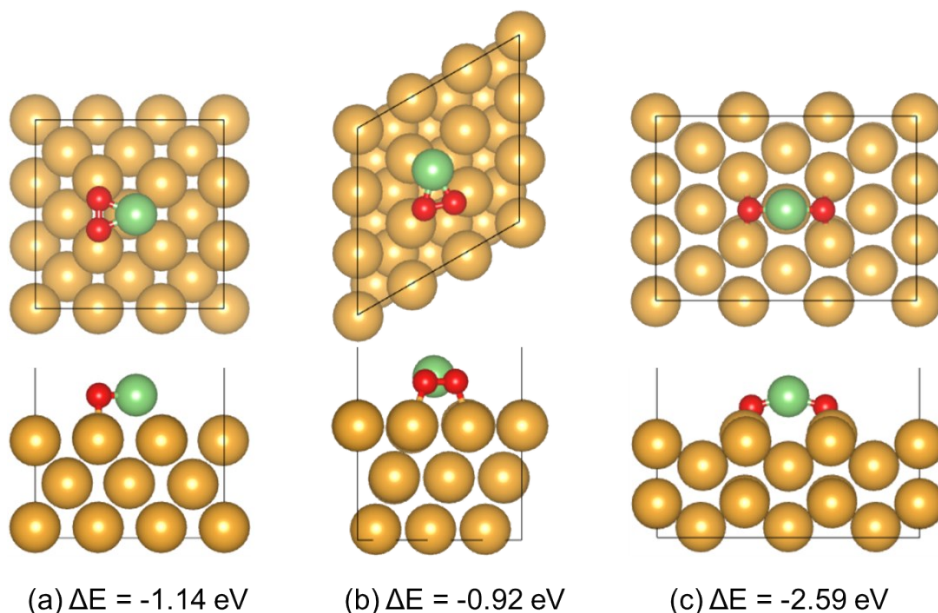


Figure S5. The most stable configurations of  $\text{LiO}_2$  adsorption on (a) Au(100), (b) Au(111) and (c) Au(110). The top views are in top panel, while the side views are in bottom panel. The Au, Li and O atoms are in gold, green and red, respectively.

The mechanism involved in Reaction (4) in Ref 6 was translated that on Au(100), the  $\text{Li}_2\text{O}_2$  formation proceeds via the electrochemical reaction in which a water molecule anchored by a  $\text{LiO}_2$  is able to activate the  $\text{O}_2$  for a two-electron reaction to form  $\text{Li}_2\text{O}_2$ . In order to model the electron transfer at an applied potential, the double-reference approach was adapted to model the double layer structure near the electrode and to determine the applied potential of the supercell.<sup>7-8</sup> The

potential at the metal/water interface was modeled by changing the number of supercell electrons. A homogeneous background charge was applied to maintain the charge neutrality of the supercell. The simulated potential (reference to Li/Li<sup>+</sup> electrode) as a function of added electron number is plotted in Figure S6. The data were fitted with linear relationship with the coefficients of determination of 0.99 and were used to determine how many electrons are needed to obtain the potential consistent with experimental value. Based on the plot in Figure S6, we choose the supercell with extra four electron to simulate the potential of 2.6 V vs Li/Li<sup>+</sup>, close to the experimental value, 2.5 V, for the discharging reactions.

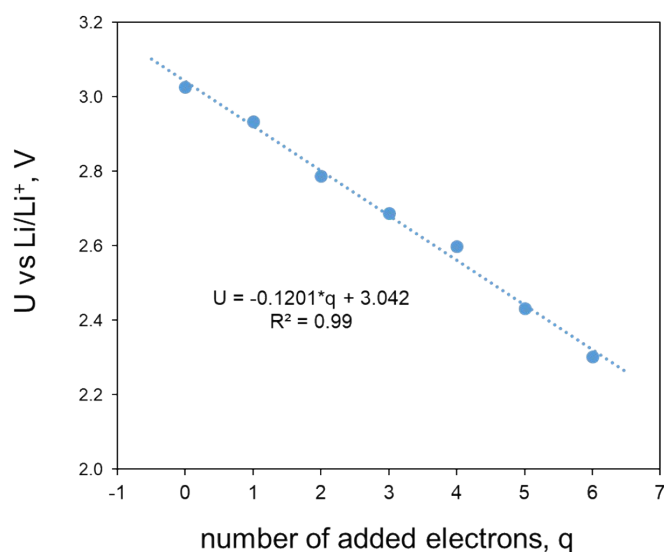


Figure S6. The linear fitted applied potential,  $U$ , with respect to Li/Li<sup>+</sup> electrode, as a function of the number of added electrons for the H<sub>2</sub>O-LiO<sub>2</sub> and O<sub>2</sub> on Au(100) with explicit DME electrolyte.

The H<sub>2</sub>O-LiO<sub>2</sub> complex and a O<sub>2</sub> molecule on Au(100) surface were optimized at 0 K, then the optimized configurations were utilized as the start point of AIMD simulations. The AIMD simulation supercell was described in Figure S7(a). The geometry of H<sub>2</sub>O-LiO<sub>2</sub> and O<sub>2</sub> on Au(100) was displayed in Figure S7(b) with hidden DME molecules for the visualization purpose. H<sub>2</sub>O-LiO<sub>2</sub> complex binds on one bridge site with one hydrogen in water pointing O<sub>2</sub> molecule with a distance of 1.94 Å. After the AIMD calculation running for 2 ps, the distance of H<sub>2</sub>O and O<sub>2</sub> becomes 2.23 Å without observation of bond elongation of O-O bond in O<sub>2</sub> or H-O bond in H<sub>2</sub>O

(see Figure S7(c)), indicating that  $\text{H}_2\text{O-LiO}_2$  did not activate  $\text{O}_2$  on Au(100) surface at current simulation time scale as suggested in Markovic's work.

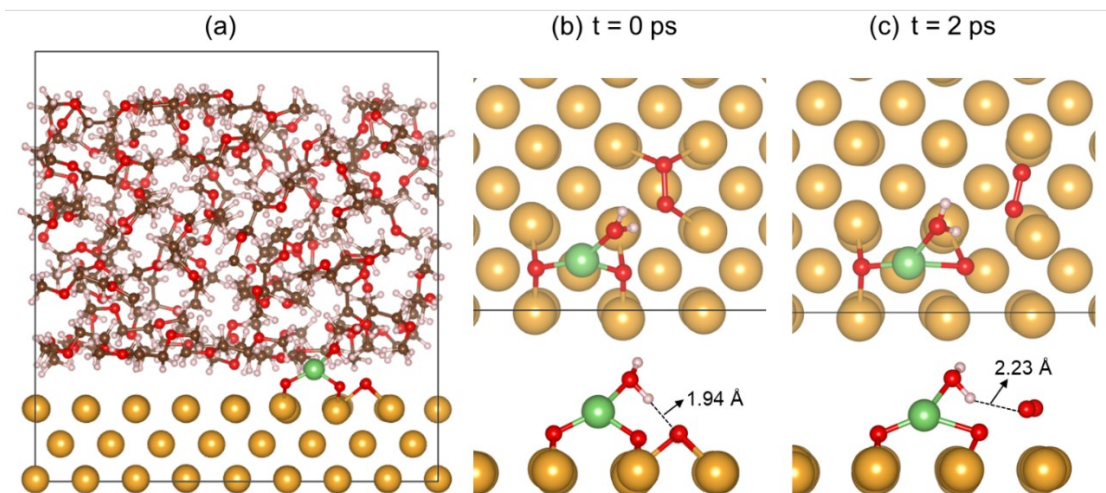


Figure S7. (a) The AIMD simulation supercell used for the discharging reaction with  $\text{H}_2\text{O-LiO}_2$  and  $\text{O}_2$  on Au(100) with explicit DME solvent. (b-c) The snapshots of reactants on Au(100) with hidden DME molecules at 0 and 2 ps with top (upper panel) and side (bottom panel) views. The Au, Li, C, O, H atoms are displayed in gold, green, brown, red and white, respectively. The blank lines represent the periodic boundaries. The distances between  $\text{H}_2\text{O}$  and  $\text{O}_2$  are labeled in (b-c).

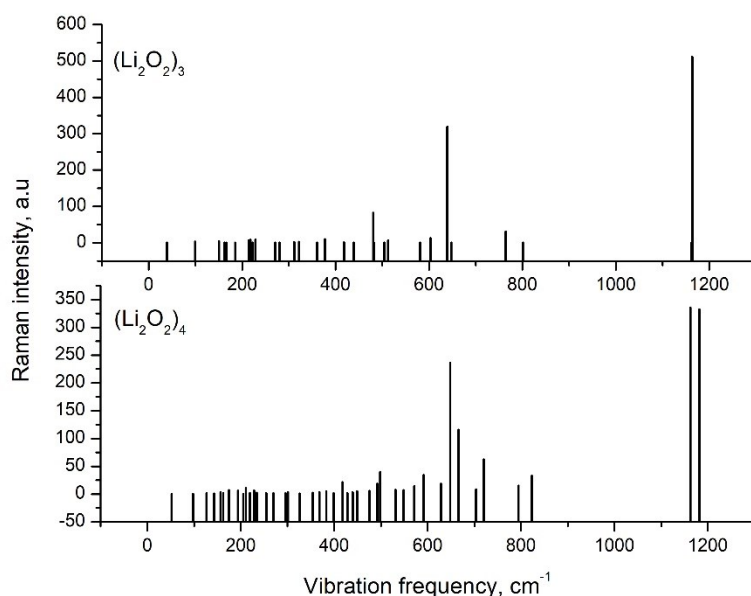


Figure S8. The calculated Raman spectra of  $(\text{Li}_2\text{O}_2)_3$  and  $(\text{Li}_2\text{O}_2)_4$  clusters using B3LYP theory with the 6-31G(2df,p) basis set.

The Raman spectra of  $(\text{Li}_2\text{O}_2)_3$  and  $(\text{Li}_2\text{O}_2)_4$  clusters were calculated using B3LYP theory with the 6-31G(2df,p) basis set, as shown in Figure S8. The obtained Raman active modes for O-O of  $\text{Li}_2\text{O}_2$  are in agreement with our previous work<sup>9</sup> (using the 6-31G(d) basis set), which was consistent with experimental measurements of Raman spectra for  $\text{Li}_2\text{O}_2$ .

1. Perdew, J. P.; Burke, K.; Ernzerhof, M., Generalized Gradient Approximation Made Simple. *Physical Review Letters* **1996**, *77*, 3865-3868.
2. Kresse, G.; Furthmüller, J., Efficient Iterative Schemes for Ab Initio Total-Energy Calculations Using a Plane-Wave Basis Set. *Physical Review B* **1996**, *54*, 11169-11186.
3. Blöchl, P. E., Projector Augmented-Wave Method. *Physical Review B* **1994**, *50*, 17953-17979.
4. Mathew, K.; Sundararaman, R.; Letchworth-Weaver, K.; Arias, T. A.; Hennig, R. G., Implicit Solvation Model for Density-Functional Study of Nanocrystal Surfaces and Reaction Pathways. *The Journal of Chemical Physics* **2014**, *140*, 084106.
5. Mathew, K.; Kolluru, V. S. C.; Mula, S.; Steinmann, S. N.; Hennig, R. G., Implicit Self-Consistent Electrolyte Model in Plane-Wave Density-Functional Theory. *The Journal of Chemical Physics* **2019**, *151*, 234101.
6. Staszak-Jirkovský, J., et al., Water as a Promoter and Catalyst for Dioxygen Electrochemistry in Aqueous and Organic Media. *ACS Catalysis* **2015**, *5*, 6600-6607.

7. Taylor, C. D.; Wasileski, S. A.; Filhol, J.-S.; Neurock, M., First Principles Reaction Modeling of the Electrochemical Interface: Consideration and Calculation of a Tunable Surface Potential from Atomic and Electronic Structure. *Physical Review B* **2006**, *73*, 165402.
8. Filhol, J.-S.; Neurock, M., Elucidation of the Electrochemical Activation of Water over Pd by First Principles. *Angewandte Chemie International Edition* **2006**, *45*, 402-406.
9. Yang, J.; Zhai, D.; Wang, H.-H.; Lau, K. C.; Schlueter, J. A.; Du, P.; Myers, D. J.; Sun, Y.-K.; Curtiss, L. A.; Amine, K., Evidence for Lithium Superoxide-Like Species in the Discharge Product of a Li–O<sub>2</sub> Battery. *Physical Chemistry Chemical Physics* **2013**, *15*, 3764-3771.